method to stain collagen fibers (in light blue) in the interstitial space. Under high-power magnification (×400), 10 nonoverlapping fields from the cortical region were selected at random and analyzed by an observer unaware of the experimental protocol. The fibrotic areas in the interstitium were highlighted on digitized images using a computer-aided manipulator (microscope) (Leitz DM IRB, software) (Quantimet 500+) (Leica, Tokyo, Japan). The fibrotic area relative to the total area of the field was calculated as a percentage. Glomeruli and large vessels were not included in the microscopic fields for image analysis. The scores of 10 fields per kidney were averaged, after which the mean scores from 12 separate animals per group were averaged.

Northern blot analysis

Renal tissue was finely minced with an autoclaved blade and immediately immersed in liquid nitrogen, and then homogenized in TRIzol reagent (Gibco BRL). RNA extraction was performed according to the manufacturer's protocol. After resuspension in Tris-EDTA buffer, 15 μg of RNA were electrophoresed in each lane in 1% agarose gels containing 2.2 mol/L formaldehyde and 0.2 mol/L 3-[N-morpholino] propane sulfonic acid (MOPS) (pH 7.0) and were transferred to a nylon membrane (Hybond N) (Amersham). The membranes were prehybridized for 1 hour at 42°C with 50% formamide, 10% Denhardt's solution, 0.1% sodium phosphate, 5 × standard saline citrate (SSC), and 180 mg/mL denatured salmon sperm DNA. They were hybridized at 42°C for overnight with cDNA probes labeled with ^{32}P-dexoycytidimine triphosphate (dCTP) by random oligonucleotide priming (RediPrime, Burlingame, CA, USA). The blots were washed in 2 × SSC, 0.1% SDS at room temperature two times for 15 minutes and in 0.2 × SSC, 0.1% SDS at 60°C two times for 10 minutes. Films were exposed at −80°C for approximately 24 hours. The density of bands for glyceraldehyde-3-phosphate dehydrogenase (GAPDH) mRNA was used to control for differences in total amount of RNA loaded onto each gel line.

Statistical analysis

All values are expressed as means ± SD. Statistical significance (defined as $P < 0.01$) was evaluated using the one-way analysis of variance (ANOVA).

RESULTS

Physiologic studies

Serum creatinine and urea nitrogen levels at the end of study were summarized in Table 1. In comparison of normal control group (serum creatinine 0.23 ± 0.04 mg/dL and urea nitrogen 24.0 ± 2.30 mg/dL), serum creatinine and urea nitrogen gave a significant rise in both CsA group and CsA/HGF group ($P < 0.05$ vs. normal control group). However, creatinine and urea nitrogen levels were higher in CsA group compared with CsA/HGF group (not significant, $P = 0.19$).

Table 1. The final concentration of serum creatinine, urea nitrogen, cyclosporine A (CsA) whole blood level, and plasma hepatocyte growth factor (HGF) in each group

Groups	Serum creatinine *mg/dL*	Urea nitrogen *mg/dL*	CsA whole blood level *ng/mL*	Plasma HGF *ng/mL*
CsA day 14	0.34 ± 0.06	33.5 ± 7.8	3667 ± 416	1.249 ± 0.138
HGF day 14	0.28 ± 0.03	25.1 ± 2.9	3200 ± 436	1.681 ± 0.076
CsA day 21	0.48 ± 0.07	54.2 ± 13.5	4275 ± 608	1.229 ± 0.076[a]
HGF day 21	0.46 ± 0.07	53.6 ± 5.8	4050 ± 420	1.578 ± 0.332

[a] $P < 0.05$ vs. CsA day 14.

Plasma concentration of HGF was measured by EIA method. In normal control rats, plasma concentration of HGF increased to 4.88 ± 0.75 ng/mL at day 3 after HGF gene transfection, and declined, reaching 0.96 ± 0.87 ng/mL and 0.47 ± 0.36 ng/mL at day 5 and day 14, respectively. Northern analysis of muscle treated with HGF gene showed that HGF mRNA expression persisted 14 days after transfection (data not shown). CsA administration increased plasma HGF levels (1.25 ± 0.14 ng/mL and 1.23 ± 0.08 ng/mL at 2 and 3 weeks, respectively); however, HGF gene transfer attained further up-rise of plasma HGF level (1.69 ± 0.08 ng/mL and 1.59 ± 0.32 ng/mL at 2 and 3 weeks, respectively).

Effect of HGF gene transfer on tubulointerstitial injury

PAS staining revealed that CsA treatment induced characteristic histologic changes by 2 weeks, including tubular atrophy and dilation, early striped fibrosis, and inflammatory cell infiltration. By 3 weeks, these lesions were more prominent and extensive with severe interstitial fibrosis (Fig. 1A). In addition, arteriolar hyalinosis was observed in CsA group (black arrow). However, HGF gene transfer alleviated these tubulointerstitial injuries (Fig. 1B), and ameliorated arteriolar hyalinosis (white arrow).

The degree of interstitial fibrosis was quantitatively assessed as fibrotic fractional volume of renal cortex using a computer-aided manipulator on Masson's trichrome–stained sections (Figs. 1C and D and 2A). CsA group showed progression of interstitial fibrosis with 5.54 ± 1.46% and 6.69 ± 1.32% at 2 and 3 weeks of CsA treatment, respectively. In parallel with the findings on tubulointerstitial injury, HGF gene transfer significantly suppressed the development of interstitial fibrosis at 2 and 3 weeks (3.86 ± 0.89% and 4.99 ± 1.46% at 2 and 3 weeks, respectively, $P < 0.01$ vs. CsA group).

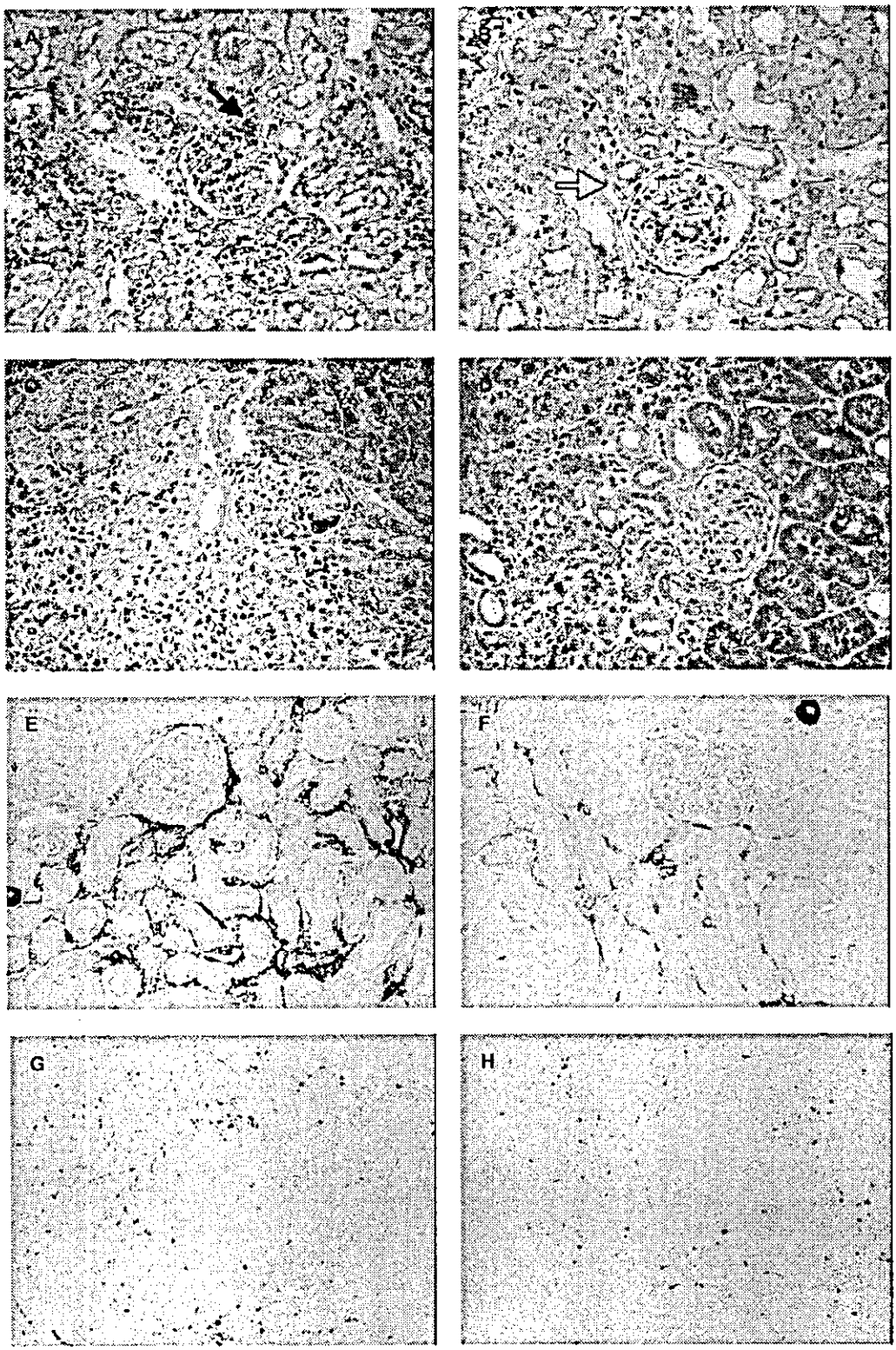

Fig. 1. Renal histopathology and immunohistochemistry. Representative photomicrographs showed the renal morphologic changes of periodic acid-Schiff (PAS) (*A* and *B*) and Masson's trichrome (*C* and *D*) staining, immunohistchemistry of alpha-smooth muscle actin (α-SMA (*E* and *F*) and ED-1 (*G* and *H*) in cyclosporine A (CsA) group (A, C, E, and G) and CsA/hepatocyte growth factor (HGF) group (B, D, G, and H) at day 21. Arteriolar hyalinosis was observed in CsA group (A, black arrow); however, HGF gene transfer ameliorated arteriolar hyalinosis (B, white arrow).

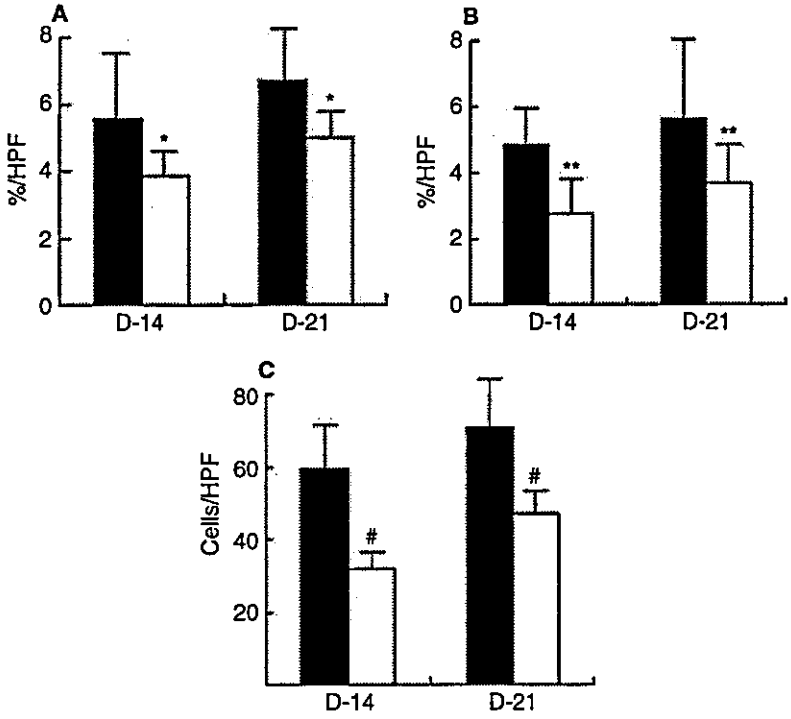

Fig. 2. Semiquantification of histologic changes. The fractional volume of interstitial fibrotic area (*A*) and alpha-smooth muscle actin (α-SMA–positive area (*B*) in the cortex (excluding glomeruli) was estimated at the field of ×400 in the minimum of 10 fields by computer-aided manipulator. ED-1–positive cells were counted at ×200 in the minimum of 10 fields (*C*). Symbols are: (■) cyclosporine (CsA groups); (□) CsA/hepatocyte growth factor (HGF) groups. Data are expressed as mean ± SD. $^{*}P < 0.01$; $^{**}P < 0.001$; $^{\#}P < 0.0001$, CsA treated group compared with CsA/HGF group.

Phenotypic alteration and macrophage infiltration

Phenotypic alteration into myofibroblast, which was estimated by immunohistochemical staining of α-SMA, leads to extracellular matrix accumulation. Upon 2 weeks treatment of CsA, a significant increase was noted in α-SMA, followed by a further increase by 3 weeks (4.86 ± 0.97% and 5.66 ± 1.67%, respectively) (Figs. 1E and 2B). Expression of α-SMA occurred in the areas of tubulointerstitial fibrosis, with most pronounced increases seen around the thickened basement membrane of the Bowman's capsule and degenerated tubules. However, progressive expression of α-SMA was significantly suppressed by the intervention with HGF gene transfer at 2 and 3 weeks (2.76 ± 1.09% and 3.71 ± 1.27%, respectively, $P < 0.0001$ vs. CsA group) (Figs. 1F and 2B).

CsA treatment induced marked and continuous infiltration of ED-1–positive macrophages throughout the experiment. Accumulation of ED-1–positive cells was observed around the damaged tubules and within the interstitium (Fig. 1G). The number of macrophages increased persistently in CsA group at 2 and 3 weeks (59.43 ± 15.15 cells per high power field and 70.53 ± 15.66 cells per high power field, respectively) (Fig. 2C). In contrast, macrophage accumulation was significantly repressed in CsA/HGF group both at 2 and 3 weeks (32.00 ± 8.70 and 45.23 ± 10.88 positive cells per high-power fields, respectively, $P < 0.001$ vs. CsA group) (Figs. 1H and 2C).

Renal tubular cell proliferation by HGF gene transfer

Ki-67 antigen is a large nuclear protein preferentially expressed during active phase of the cell cycle (G_1, S, G_2, and M phases), but absent in resting cells (G_0) and its antibody is valuable by allowing direct monitoring of the growth fraction of normal and neoplastic cells. To assess the regeneration of tubular epithelial cells, cortical Ki-67–positive tubular cells were counted at ×200 magnification in the minimum of 10 fields. Ki-67–positive cells were few in normal kidney (1.00 ± 1.17) (Fig. 3A), but significantly increased in CsA group at 2 weeks and 3 weeks (6.54 ± 2.11 and 6.31 ± 2.55, respectively, $P < 0.0001$ vs. normal control) (Fig. 3B and D). HGF gene transfer showed further increased Ki-67–positive cells (8.92 ± 2.43 at 2 weeks, $P = 0.006$, and 10.41 ± 3.48 at 3 weeks, $P < 0.0001$ vs CsA group) (Fig. 3C and D). Of interest is that Ki-67–positive cells existed mainly in damaged interstitial lesions in CsA-treated kidney (Fig. 3B, left area), while Ki-67–positive cells were observed in tubular epithelial cells, but not in interstitium in HGF group.

Morphologic evidence of apoptosis

To investigate whether HGF gene transfection could protect the tubular apoptosis, we examined the apoptotic bodies, marked as an in situ end-labeled DNA fragment with the TUNEL method. In parallel with the tubulointerstitial damage, tubular apoptosis was persistently

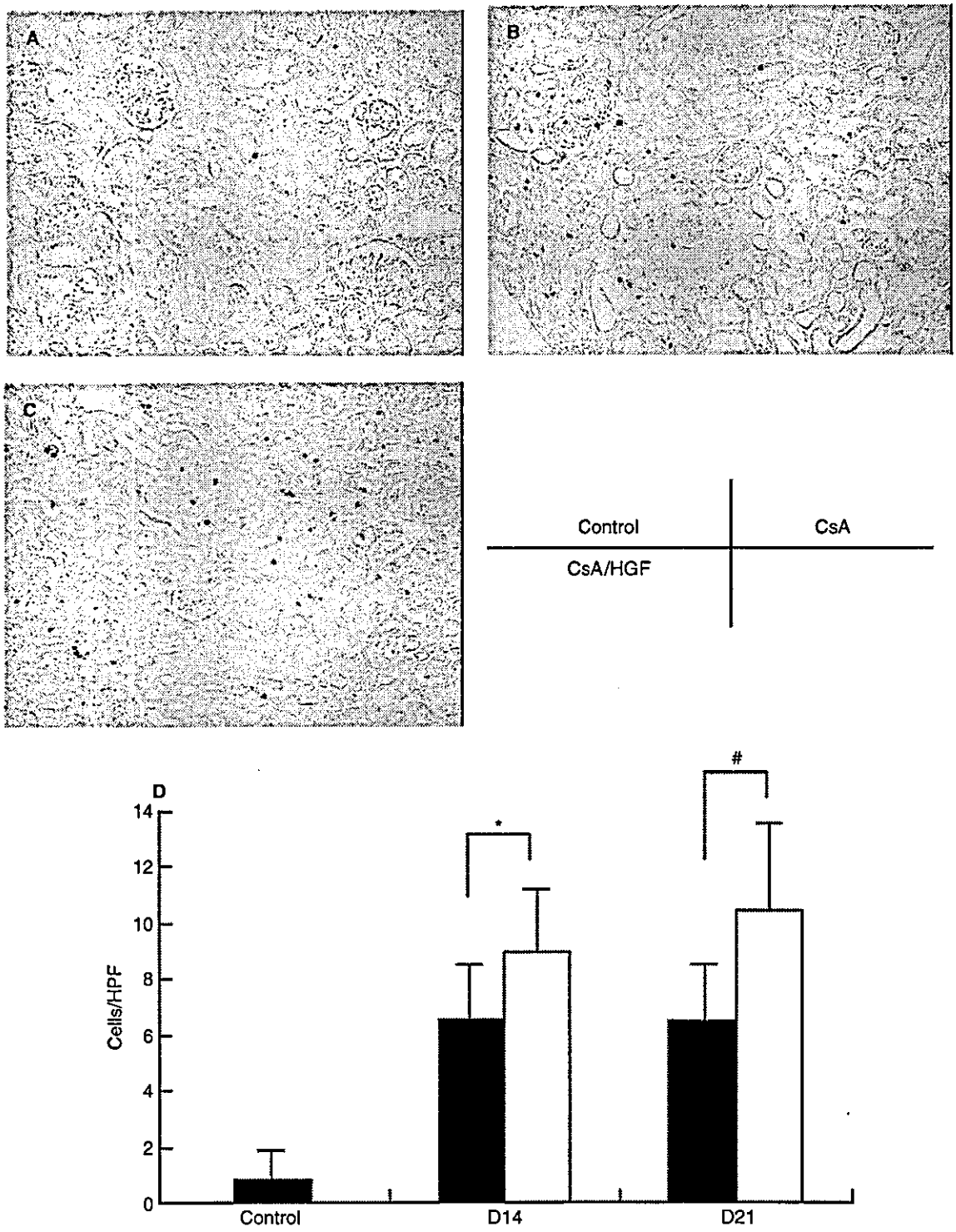

Fig. 3. Renal tubular cell proliferation. Representative photographs showed immunohistochemical staining of Ki-67 antigen, a cell proliferation marker, in normal kidney (*A*), cyclosporine A (CsA) group (*B*), and CsA/hepatocyte growth factor (HGF) group (*C*). Ki-67–positive renal tubular cells also increased in CsA treatment group, but further increase was shown in CsA/HGF group. Proliferative cells were mainly observed in damaged interstitial lesions in CsA-treated kidney (B, arrow). Ki-67–positive cells were counted at ×200 in the minimum of 10 fields at day 14 and 21 (*D*). Symbols are: (■) CsA groups; (□) CsA/HGF groups. Data are expressed as mean ± SD. $^{*}P < 0.01$; $^{\#}P < 0.001$.

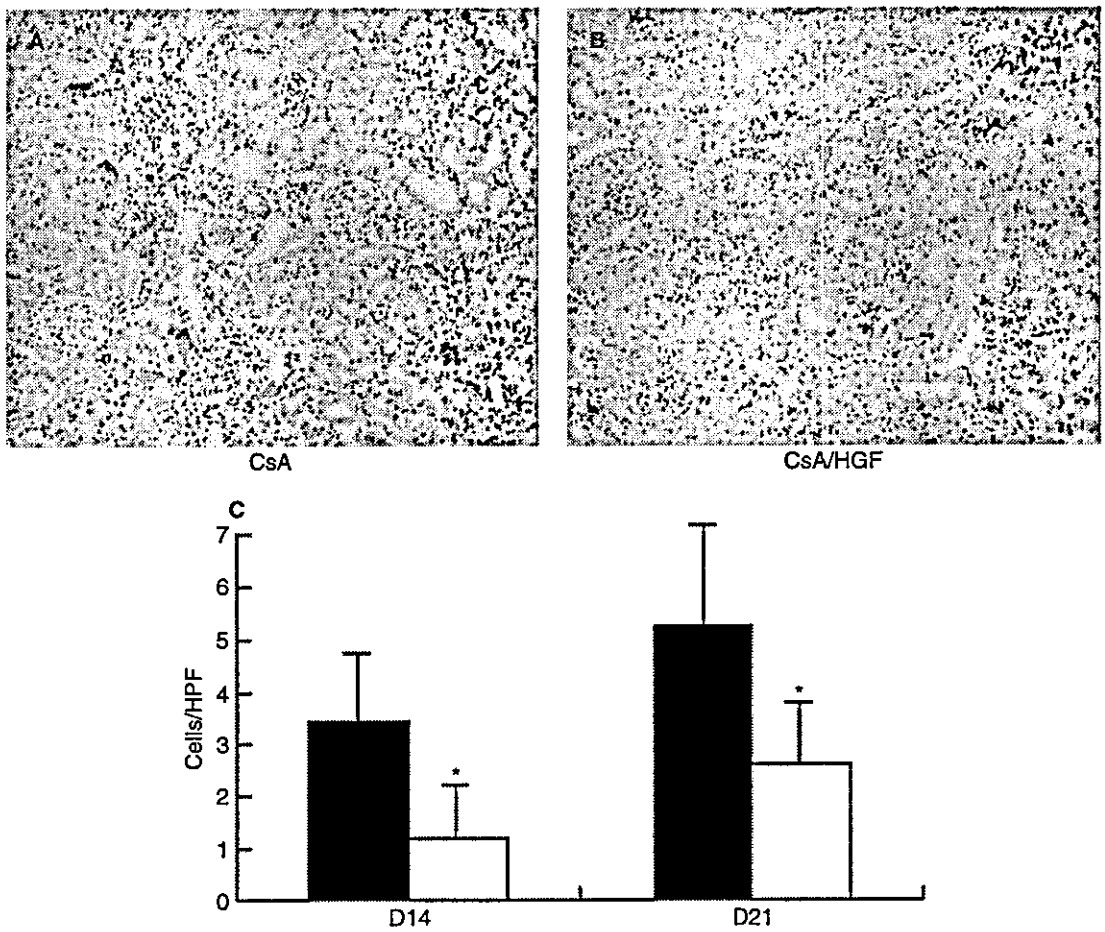

Fig. 4. Apoptosis detected by terminal deoxynucleotidyl transferase (TdT)-mediated deoxyuridine triphosphate (dUTP) nick end labeling (TUNEL) assay. TUNEL-positive cells (green arrows) were often detected in the cortical area in cyclosporine A (CsA) administration for 3 weeks (*A*), and these were suppressed by hepatocyte growth factor (HGF) gene transfer (*B*). The scores of TUNEL positive cells were counted in the cortical tubular cells at ×200 magnification in the minimum of 10 fields at day 14 and 21 (*C*). Symbols are: (■) CsA groups; (□) CsA/HGF groups. Data are expressed as mean ± SD. $^*P < 0.001$.

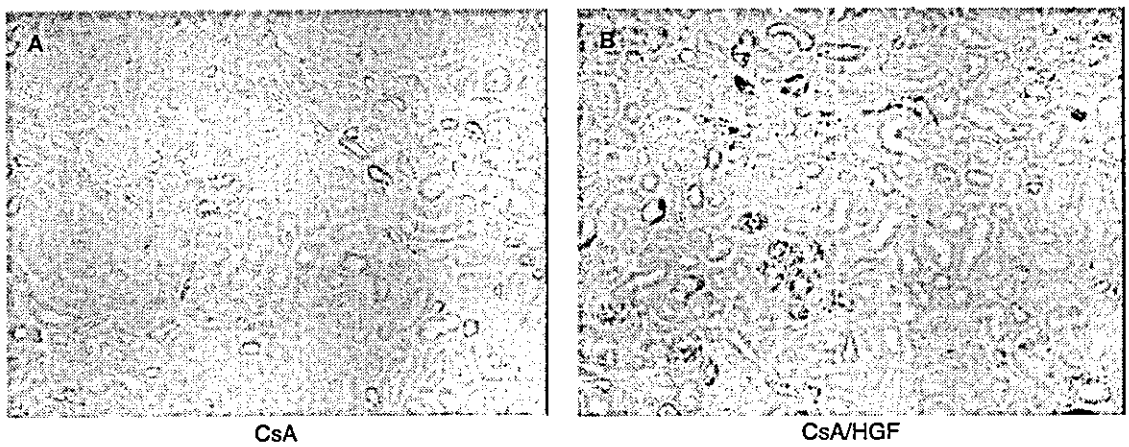

Fig. 5. Immunohistochemical staining of phosphorylated Bad. In normal kidneys, the phosphorylated-Bad was not detectable by immunohistochemstry. After the induction of cyclosporine A (CsA) treatment, obvious but weak phosphorylated Bad staining was present (*A*). In hepatocyte growth factor (HGF)-treated kidney phsophorylated Bad was abundantly up-regulated (*B*).

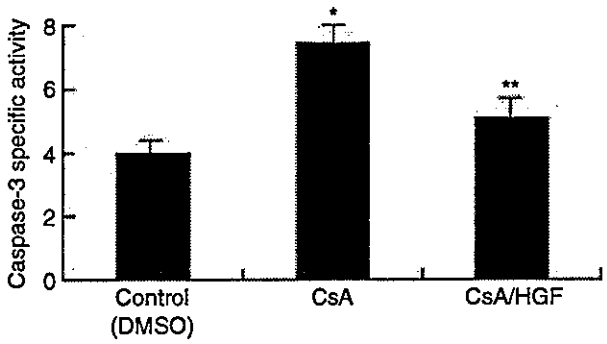

Fig. 6. Changes of caspase-3 activity. HK-2 cells were treated with cyclosporine (CsA) (40 μmol/L) for 24 hours with or without hepatocyte growth factor (HGF) (50 ng/mL) pretreatment for 1 hour. Experiments were performed in ternary. Caspase-specific activity was calculated by constructing of pNA (p-nitroaniline) caliblation curve and applying the value of absorbance OD405. The number of Y axis represents pmol pNA liberated per hour/μg protein. Data are expressed as mean ± SD. $^{*}P < 0.005$ CsA group compared with control group; $^{**}P < 0.01$ CsA/HGF group compared with CsA group. DMSO is dimethyl sulfoxide.

increased at 2 and 3 weeks after CsA treatment (3.45 and 5.25 cells per high power field, respectively) (Fig. 4A and C), while HGF significantly inhibited tubular apoptosis (1.2 and 2.65 cells per high power field, respectively, $P <$ 0.001 vs. CsA group) (Fig. 4B).

As we determined that HGF gene therapy could successfully inhibit apoptosis in CsA-induced tubulointerstitial injury, we examined the possible mechanism of apoptosis by staining the phosphorylated-Bad expression. Bad promotes apoptosis in part through heterodimerization with the survival proteins Bcl-2 and Bcl-x_L. Phosphorylation of Bad prevents this apoptosis. In normal kidneys, the phosphorylated-Bad was not detectable by immunohistochemstry. After the induction of CsA treatment, obvious but weak phosphorylated Bad staining was present (Fig. 5A). In HGF-treated kidney phsophorylated Bad was abundantly up-regulated (Fig. 5B).

Caspase-3 activity assay in HK-2 cells

In order to provide direct evidence for caspase activation, we investigated the activity of caspase-3 in human proximal tubular epitherial (HK-2) cells. Caspase-3 activity was up-regulated only under the exposure of 0.1% DMSO (3.98 ± 0.11) as the control group, and showed significant increase by CsA treatment (7.44 ± 0.39, $P < 0.005$ vs. control). However, HGF pretreatment significantly inhibited the CsA-induced up-regulation of caspase-3 activity (5.10 ± 0.49, $P < 0.01$ vs. CsA group) (Fig. 6).

Western immunoblot analysis on HK-2 cells

To demonstrate the mechanism of apoptosis inhibition by HGF, we performed Western immunoblot analysis of phosphorylated-Akt, Bcl-2, and Bax proteins (Fig. 7A). Western blot analysis showed that CsA treatment reduced Bcl-2 protein level to 0.57 ± 0.10 of that in untreated HK-2 cells. However, additional treatment with HGF recovered the expression of Bcl-2 protein to 0.97 ± 0.19 of that in untreated HK-2 cells (Fig. 7B). In addition, the treatment of HGF significantly increased the phosphorylation of Akt in CsA-treated cultured cells (the relative ratio of phosphorylated Akt signals to Akt signals $4.27 \pm 0.11 \times 10^{-2}$ in HGF/CsA vs. $2.78 \pm 0.39 \times 10^{-2}$ in CsA, $P < 0.05$) (Fig. 7C). Neither CsA nor HGF affected Bax expression (data not shown). Total Akt protein levels were similar in all groups. However, Akt phosphrylation, an active form of Akt, was suppressed by CsA, but was increased by HGF.

Northern blot

Northern analysis was performed of renal cortex in each of four groups. The cortical mRNA expression of TGF-β was up-regulated in CsA group by day 14 compared with normal control group, while HGF treatment significantly reduced TGF-β mRNA expression (ratios of TGF-β signal to GAPDH signal 0.168 ± 0.007 in CsA group vs. 0.091 ± 0.002 in CsA/HGF group, $P < 0.01$). The inhibitory effect on TGF-β was also observed at day 21.

DISCUSSION

In the present study, we found that HGF gene transfer into muscle using electroporation had a protective effect on chronic CsA-induced nephrotoxicity. Here, we demonstrated that HGF gene transfer reduced CsA-induced tubulointerstitial injury. Tubular epithelial apoptosis was suppressed and macrophage infiltration, phenotypic alteration of interstitial myofibroblasts, and interstitial fibrosis were also restricted in HGF group.

Several reports indicated the involvement of HGF in renal regeneration [10, 19]. Rapid increases in HGF mRNA and/or protein levels in the kidney and plasma were observed in various types of renal injury induced by nephrotoxins, renal ischemia, and ureteral obstruction [10]. Recently, it has been reported that endogenous as well as exogenous HGF prevents renal fibrosis in a mouse model of nephritic syndrome [20]. The present study obtained three major findings: (*1*) exogenous supply of HGF provided effective protection from tubular apoptosis caused by CsA treatment in vitro and in vivo; (*2*) HGF gene transfer induced tubular cell proliferation; and (*3*) HGF gene transfection suppressed the expression of TGF-β followed by the inhibition of interstitial fibrosis.

We showed the therapeutic effects of HGF transgene approach on CsA-induced tubular epithelial injury. PAS staining revealed that CsA treatment induced tubular

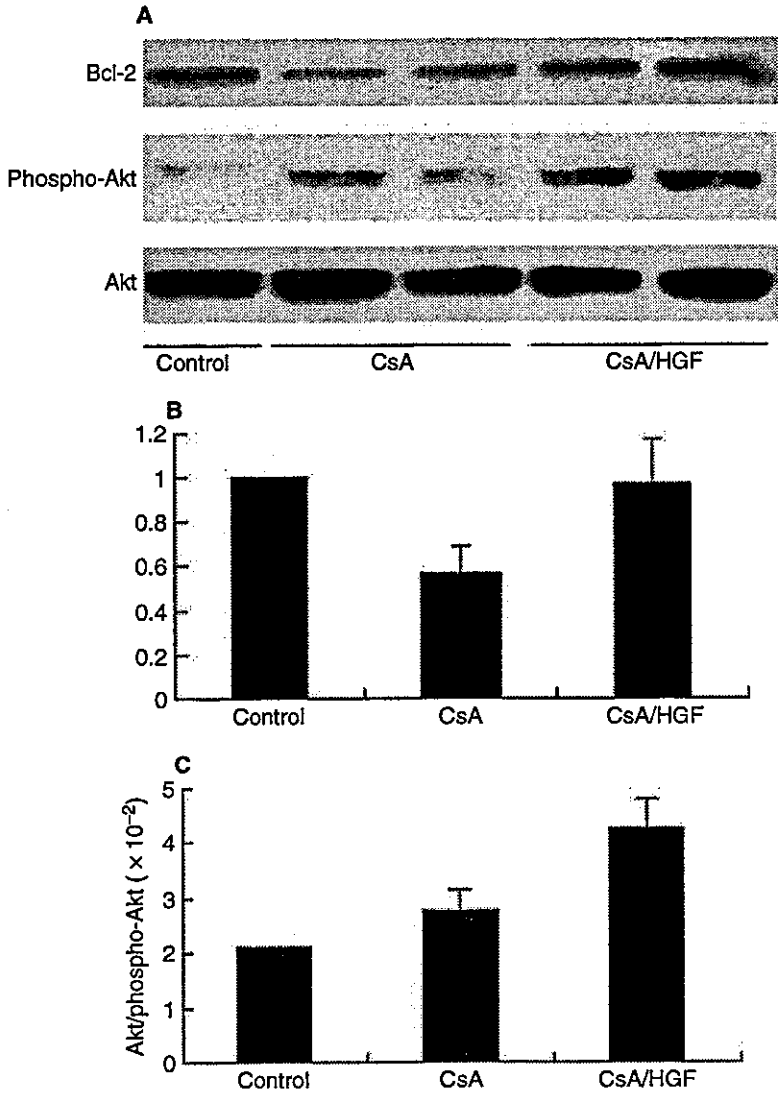

Fig. 7. The protective mechanism of hepatocyte growth factor (HGF) from apoptosis in HK-2 cells. (*A*) Western immunoblot of HK-2 cells for the treatment of 0.1% dimethy sulfoxide (DMSO) used as control (left), 40 mmol/L cyclosporine A (CsA) in 0.1% DMSO for 24 hours (middle), 40 mmol/L CsA in 0.1% DMSO for 24 hours before 1-hour treatment of 50 ng/mL HGF (right). Graphic presentations represent quantitative abundance of bcl-2 expression levels (*B*) and phospho-Akt/Akt ratio (*C*).

atrophy and dilatation; however, HGF gene transfer ameliorated these observations. In parallel with the tubular injury, tubular apoptosis was persistently increased at 2 and 3 weeks after CsA treatment, while HGF significantly inhibited tubular apoptosis. In addition, Ki-67 staining showed that HGF gene transfer significantly increased the number of proliferating tubular epithelial cells. Of interest is that HGF treatment did not accelerate the proliferation of interstitial myofibroblasts, while Ki-67–positive cells were likely to be limited to damaged interstitial lesion of CsA-treated kidney. To address whether HGF gene transfer affects normal kidney, we transferred HGF gene into the muscle of normal rats. We observed no histologic changes (tubular apoptosis or interstitial infiltration) in HGF gene-treated normal kidney. However, cortical Ki-67–positive tubular epithelial cells were significantly increased on day 3 and sustained until day 14 (Fig. 9). This observation supports the previous report that HGF promotes DNA synthesis of tubular epithelial cells [21]. These results emphasized the protective effect of HGF gene transfer on the balance of tubular cell proliferation and apoptosis in CsA-induced tubulointerstitial injury.

In this study, we also showed that HGF supplementation inhibited CsA-induced arteriolar hyalinosis. Arteriolar hyalinosis induced by CsA is a well-described but poorly characterized lesion. Although it has been commonly known that the chronic form of CsA injury is a consequence of CsA-induced arteriolar vasoconstriction of vascular smooth muscle cells, the development of arteriolar hyalinosis may be due to direct toxicity of CsA, rather than a hemodynamic consequence. The precise mechanism why HGF gene transfer suppressed arteriolar hyalinosis remains unclear in this study. However, we observed

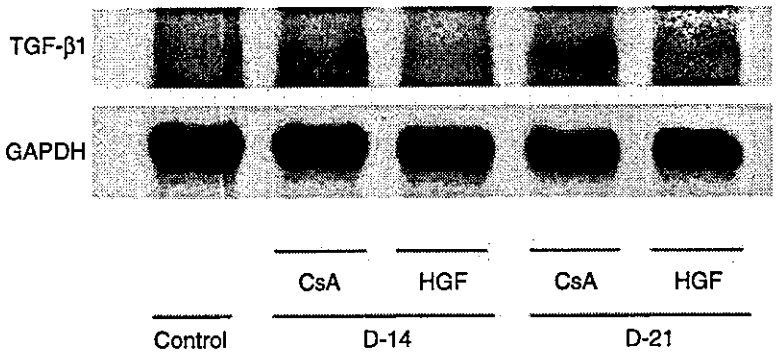

Fig. 8. Northern analysis of renal cortex. Northern analysis showed the representative cortical mRNA levels of transforming growth factor-β (TGF-β) and glyceraldehyde-3-phosphate dehydrogenase (GAPDH) in normal control kidney and cyclosporine A (CsA)-treated and hepatocyte growth factor (HGF) gene-transferred rats at days 14 and 21.

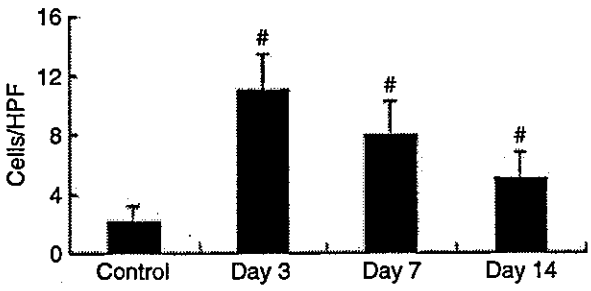

Fig. 9. Effect of hepatocyte growth factor (HGF) gene transfer in normal rat kidney: Cortical Ki-67–positive tubular epithelial cells were counted for the time course. Ki-67–positive cells were significantly increased at 3 days after HGF gene transfer and sustained until day 14. $^{\#}P < 0.001$ vs. normal group.

no changes in systemic blood pressure after HGF gene transfer. Therefore, suppression of arteriolar hyalinosis is not due to the direct influence of systemic hemodynamics. However, it is possible that HGF may affect the renal hemodynamics via the escape from tubular apoptosis and interstitial fibrosis. The recent study demonstrates that low CsA doses generated interstitial fibrosis with arteriolar hyalinosis, possibly through macrophage infiltration and increased TGF-β expression [22]. In addition, it was reported that local HGF secretion from vascular cells was negatively regulated by TGF-β [23]. According to this notion, the supplementation of HGF inhibited the arteriolar hyalynosis and improved renal blood flow, thereby protecting tubular cells from ischemic injury.

Another mechanism of the suppression in tubulointerstitial injury may be associated with anti-apoptotic effect of HGF on renal epithelial cells, which is partly mediated by the induction of the phosphorylation of Akt. We demonstrated that HGF supplementation induced the phosphorylation of Akt in vitro tubular epithelial cells. Activation of Akt has been shown to protect a wide variety of cells from apoptosis. It is reported that Akt is rapidly activated during liver regeneration and that activation of Akt protects hepatocyte from TGF-β–induced apoptosis in vitro [24]. Several downstream targets of Akt (such as E2F, c-myc, and Bad) have been implicated in cell cycle progression and antiapoptosis [25]. Among these, the phosphorylation of Bad and its consequent dissociation from Bcl-x_L is the most important signaling event linked to the anti-apoptotic effect of Akt [26]. Treatment of tubular epithelial cells with CsA inactivated Akt, while HGF treatment recovered them from its inactivation. We further examined the effect of HGF on the phosphorylation of Bad in CsA-treated kidney. Immunohistochemistry revealed that phosphorylated Bad increased in tubular epithelial cells in HGF-treated kidney, suggesting that HGF gene transfer activated Akt-Bad cascade. The role of Bcl-2 and Bax in the process of apoptosis has been widely investigated. It is postulated that Bcl-2 and Bax are a pair of homologous proteins having inverse effects on cell growth and cell death. Bcl-2 serves as an inhibitor of apoptosis, while Bax acts as a proapoptotic antagonist against the cell survival effect of Bcl-2. However, there are only limited data regarding Bcl-2 regulation in CsA nephrotoxicity. Our data showed that Bcl-2 is diminished in CsA-treated tubular epithelial cells, while HGF supplementation increased Bcl-2 expression. Neither CsA nor HGF affected the Bax expression (data not shown). In current study, we found that HGF treatment directly inhibited caspase-3 activity correlated with the up-regulation of Bcl-2. Our finding further confirms that HGF may execute the anti-apoptotic function by enhancing the phosphorylation of Akt and Bcl-2.

TGF-β is a fibrotic cytokine and plays an important role in CsA-induced accumulation of extracellular matrix protein. The role of TGF-β in mediating CsA nephrotoxicity has been evaluated in several studies. CsA has been shown to up-regulate TGF-β expression in murine tubular cells and tubulointerstitial fibroblasts [27]. In patients with chronic allograft nephropathy and CsA-nephrotoxicity, there is increased TGF-β production [28]. Neutralizing TGF-β antibody prevents matrix synthesis and attenuates renal injury and renal function in CsA nephrotoxicity [22]. A reciprocal change in the expression of TGF-β and HGF was noted during the onset of

tubulointerstitial fibrosis caused by unilateral ureter ligated obstruction in mice [14]. We observed the increase of plasma HGF by CsA treatment (1.25 ± 0.14 ng/mL and 1.23 ± 0.08 ng/mL at 2 and 3 weeks, respectively). However, continuous renal tissue injury and persistent expression of TGF-β may lead decrease of endogenous HGF and result in irreversible renal insufficiency. In this study, HGF gene transfer attained further up-rise of plasma HGF level (1.69 ± 0.08 ng/mL and 1.59 ± 0.32 ng/mL at 2 and 3 weeks, respectively) that indicated to play several roles against renal damage beyond physiological level. In addition, HGF gene transfer decreased TGF-β mRNA levels in CsA-treated kidney. HGF prevents epithelial cell death and remodeling of renal tissue with injury or fibrosis, which is completely opposite role of TGF-β. Therefore, exogenous HGF supplement could be a therapeutic target against renal injury. In fact, several studies demonstrate that HGF has preventive and therapeutic effects in cases of acute and chronic renal failure/renal fibrosis in laboratory animals. It is unclear whether HGF suppresses TGF-β expression directly or indirectly, but the supplement of HGF results in suppression of TGF-β expression and enhances remodeling of renal tissues. These results support the hypothesis that the counterbalance between TGF-β and HGF has determinant role in the pathogenesis and therapeutics of a fibrosis related diseases.

We used gene transfer approach instead of recombinant protein for the following reasons. First, since the half life of HGF is quite short, recombinant HGF treatment requires a huge dose of recombinant protein and frequent injections. Second, administered high dose of HGF protein may cause adverse effects. Finally, recombinant protein is costly. On the contrary, gene transfer is simple, safe, cheap, and needs less frequent injections. Here, we adopted electroporation-mediated gene transfer into muscle. Recently, gene transfer by electroporation in vivo has been demonstrated to be effective for introducing DNA into mouse muscle [29]. We also demonstrated that PDGFR/Fc gene transfer by the electroporation into skeletal muscle resulted in a significant increase in the protein level [16]. In addition, regenerating muscle by treatment with bupivacaine prior to the transfection produced 80-fold or more increased gene expression at protein level [30].

CONCLUSION

We demonstrated that HGF gene transfer reduced CsA-induced tubulointerstitial injury in two ways; protection of tubular epithelial cells and inhibition of interstitial fibrosis. It is speculated that electroporation-mediated HGF gene transfer has value in treating chronic CsA-induced nephrotoxicity.

Reprint requests to Dr. Yoshitaka Isaka, Department of Internal Medicine and Therapeutics, Osaka University Graduate School of Medicine, Suita 565-0871, Japan.
E-mail: kidney@medone.med.osaka-u.ac.jp

REFERENCES

1. Bennett WM: Insights into chronic cyclosporine nephrotoxicity. *Int J Clin Pharmacol Ther* 34:515–519, 1996
2. Opelz G, Dohler B: Cyclosporine and long-term kidney graft survival. *Transplantation* 72:1267–1273, 2001
3. Andoh TF, Bennett WM: Chronic cyclosporine nephrotoxicity. *Curr Opin Nephrol Hypertens* 7:265–270, 1998
4. Shihab FS: Cyclosporine nephropathy: Pathophysiology and clinical impact. *Semin Nephrol* 16:536–547, 1996
5. Myers BD, Ross J, Newton L, *et al*: Cyclosporine-associated chronic nephropathy. *N Engl J Med* 311:699–705, 1984
6. Thomas SE, Andoh TF, Pichler RH, *et al*: Accelerated apoptosis characterizes cyclosporine-associated interstitial fibrosis. *Kidney Int* 53:897–908, 1998
7. Shihab FS, Andoh TF, Tanner AM, *et al*: Role of transforming growth factor-beta 1 in experimental chronic cyclosporine nephropathy. *Kidney Int* 49:1141–1151, 1996
8. Nakamura T, Nishizawa T, Hagiya M, *et al*: Molecular cloning and expression of human hepatocyte growth factor. *Nature* 342:440–443, 1989
9. Nakamura T, Teramoto H, Ichihara A: Purification and characterization of a growth factor from rat platelets for mature parenchymal hepatocytes in primary cultures. *Proc Natl Acad Sci USA* 83:6489–6493, 1986
10. Matsumoto K, Nakamura T: Hepatocyte growth factor: Renotropic role and potential therapeutics for renal diseases. *Kidney Int* 59:2023–2038, 2001
11. Amaike H, Matsumoto K, Oka T, *et al*: Preventive effect of hepatocyte growth factor on acute side effects of cyclosporin A in mice. *Cytokine* 8:387–394, 1996
12. Miller SB, Martin DR, Kissane J, *et al*: Hepatocyte growth factor accelerates recovery from acute ischemic renal injury in rats. *Am J Physiol* 266:F129–F134, 1994
13. Liu Y: Hepatocyte growth factor promotes renal epithelial cell survival by dual mechanisms. *Am J Physiol* 277:F624–F633, 1999
14. Mizuno S, Matsumoto K, Nakamura T: Hepatocyte growth factor suppresses interstitial fibrosis in a mouse model of obstructive nephropathy. *Kidney Int* 59:1304–1314, 2001
15. Liu ML, Mars WM, Zarnegar R, *et al*: Uptake and distribution of hepatocyte growth factor in normal and regenerating adult rat liver. *Am J Pathol* 144:129–140, 1994
16. Nakamura H, Isaka Y, Tsujie M, *et al*: Electroporation-mediated PDGF receptor-IgG chimera gene transfer ameliorates experimental glomerulonephritis. *Kidney Int* 59:2134–2145, 2001
17. Tsujie M, Isaka Y, Nakamura H, *et al*: Electroporation-mediated gene transfer that targets glomeruli. *J Am Soc Nephrol* 12:949–954, 2001
18. Nakamura H, Isaka Y, Tsujie M, *et al*: Introduction of DNA enzyme for Egr-1 into tubulointerstitial fibroblasts by electroporation reduced interstitial alpha-smooth muscle actin expression and fibrosis in unilateral ureteral obstruction (UUO) rats. *Gene Ther* 9:495–502, 2002
19. Igawa T, Matsumoto K, Kanda S, *et al*: Hepatocyte growth factor may function as a renotropic factor for regeneration in rats with acute renal injury. *Am J Physiol* 265:F61–F69, 1993
20. Mizuno S, Kurosawa T, Matsumoto K, *et al*: Hepatocyte growth factor prevents renal fibrosis and dysfunction in a mouse model of chronic renal disease. *J Clin Invest* 101:1827–1834, 1998
21. Ishibashi K, Sasaki S, Sakamoto H, *et al*: Hepatocyte growth factor is a paracrine factor for renal epithelial cells: Stimulation of DNA synthesis and NA,K-ATPase activity. *Biochem Biophys Res Commun* 182:960–965, 1992
22. Islam M, Burke JF, Jr., McGowan TA, *et al*: Effect of anti-transforming growth factor-beta antibodies in cyclosporine-induced renal dysfunction. *Kidney Int* 59:498–506, 2001
23. Nakano N, Morishita R, Moriguchi A, *et al*: Negative regulation

of local hepatocyte growth factor expression by angiotensin II and transforming growth factor-beta in blood vessels: Potential role of HGF in cardiovascular disease. *Hypertension* 32:444–451, 1998
24. HONG F, NGUYEN VA, SHEN X, *et al*: Rapid activation of protein kinase B/Akt has a key role in antiapoptotic signaling during liver regeneration. *Biochem Biophys Res Commun* 279:974–979, 2000
25. DATTA SR, BRUNET A, GREENBERG ME: Cellular survival: A play in three Akts. *Genes Dev* 13:2905–2927, 1999
26. DATTA SR, DUDEK H, TAO X, *et al*: Akt phosphorylation of BAD couples survival signals to the cell-intrinsic death machinery. *Cell* 91:231–241, 1997
27. WOLF G, THAISS F, STAHL RA: Cyclosporine stimulates expression of transforming growth factor-beta in renal cells. Possible mechanism of cyclosporines antiproliferative effects. *Transplantation* 60:237–241, 1995
28. SHIHAB FS, YAMAMOTO T, NAST CC, *et al*: Transforming growth factor-beta and matrix protein expression in acute and chronic rejection of human renal allografts. *J Am Soc Nephrol* 6:286–294, 1995
29. AHARA H, MIYAZAKI J: Gene transfer into muscle by electroporation in vivo. *Nat Biotechnol* 16:867–870, 1998
30. VITADELLO M, SCHIAFFINO MV, PICARD A, *et al*: Gene transfer in regenerating muscle. *Hum Gene Ther* 5:11–18, 1994

Kidney International, Vol. 65 (2004), pp. 2228–2237

Role of mast cells in the development of renal fibrosis: Use of mast cell–deficient rats

SHINOBU MIYAZAWA, OSAMU HOTTA, NAOKO DOI, YUMIKO NATORI, KIYOTAKA NISHIKAWA, and YASUHIRO NATORI

Department of Clinical Pharmacology, Research Institute, International Medical Center of Japan, Tokyo, Japan; Department of Nephrology, Sendai Shakaihoken Hospital, Sendai, Japan

Role of mast cells in the development of renal fibrosis: Use of mast cell–deficient rats.

Background. Recent clinical studies have shown that the number of interstitial mast cells increases in various types of renal disease and correlates well with the magnitude of interstitial fibrosis. The present study was conducted to assess the role of mast cells in renal fibrosis by examining an experimental glomerular disease.

Methods. A rat model of chronic glomerular disease, puromycin aminonucleoside-nephrosis, was induced in mast cell–deficient (*Ws/Ws*) and normal (+/+) rats.

Results. The area of interstitial fibrosis was widely distributed at 6 weeks in both groups of rats; however, unexpectedly, the area of interstitial fibrosis was greater in *Ws/Ws* rats than in +/+ littermates. Biochemical analysis of the hydroxyproline content confirmed the more severe fibrosis in the *Ws/Ws* rats. The number of mast cells increased in both *Ws/Ws* and +/+ rats, concomitant with the development of interstitial fibrosis, but was confirmed to be lower in *Ws/Ws* than in +/+ rats. There were no differences in the numbers of interstitial macrophages and T lymphocytes between the two groups. Reverse transcription-polymerase chain reaction analysis of cytokine expression revealed that the level of mRNA for transforming growth factor-β (TGF-β), a potent profibrotic cytokine, was higher in *Ws/Ws* rats. In addition, heparin, one of the major components of mast cells, inhibited the expression of TGF-β mRNA in rat fibroblasts in culture.

Conclusion. These results suggest that mast cells do not play a major role in the pathogenesis of interstitial fibrosis in puromycin aminonucleoside nephrosis. Rather, they might be protective or ameliorative in this model through the inhibition of TGF-β production by heparin, and possibly in other models and also in humans.

Mast cells are known to be immune-effector cells that augment inflammatory reactions. It is widely accepted that mast cells are involved in a number of allergic inflammatory diseases as well as in host defense against pathogens. In addition, several lines of evidence suggest that mast cells may participate in fibrotic processes. Mast cells are found in fibrogenic lesions in various tissues in human diseases, such as pulmonary fibrosis [1, 2], hepatic cirrhosis [3, 4], scleroderma [5, 6], and keloid [7]. Mast cells serve as a rich source of several mediators [8], including histamines, proteoglycans, and proteolytic enzymes (proteases), as well as a number of cytokines [9], some of which are reported to be mitogenic [10] and chemotactic [11] for fibroblasts, and to stimulate the production of the extracellular matrix (ECM) by fibroblasts [9, 10, 12]. Furthermore, mast cells themselves produce components of the ECM [13]. Therefore, for these reasons they are considered to play a profibrogenic role in the above-mentioned diseases.

In recent years, mast cells were shown to be present in the interstitial area of human renal biopsy tissues from patients with various renal diseases, such as IgA nephropathy [14–16], rapidly progressive glomerulonephritis [17], focal and segmental glomerulosclerosis [15], diabetic nephropathy [15, 18], and kidney graft rejection [16, 19, 20]. Furthermore, the number of interstitial mast cells in these glomerular diseases correlates well with the degree of interstitial fibrosis. Tubulointerstitial lesions including interstitial fibrosis are considered to be prognostic features of various glomerular diseases; regardless of its primary causes, decreased renal function correlates most closely with pathologic changes in the tubulointerstitium, which include interstitial fibrosis, tubular atrophy, and loss of peritubular capillaries [21, 22]. Based on these observations, mast cells are suggested to contribute to the renal deterioration in glomerular diseases by inducing interstitial fibrosis [14, 15, 17]. However, there have been no studies that directly show the involvement of mast cells in the pathogenesis of interstitial fibrosis in the kidney.

To elucidate the role of mast cells in the interstitial fibrosis in progressive glomerular diseases, we

Key words: mast cell, *Ws/Ws rat*, renal fibrosis, animal model, transforming growth factor-β.

Received for publication January 26, 2003
and in revised form September 5, 2003, and December 11, 2003
Accepted for publication January 15, 2004

investigated the accumulation of mast cells in an animal model of glomerular disease that is accompanied by interstitial fibrosis and renal deterioration. Furthermore, we utilized mast cell–deficient *Ws/Ws* rats to test if mast cells contribute to the development of the interstitial fibrosis. *Ws/Ws* rats have very few mast cells in their skin and other tissues [less than 1% of the number in control (+/+) littermates] because of a small deletion in the tyrosine kinase domain of the *c-kit* gene [23–25]. Unexpectedly, in this study we found that the degree of interstitial fibrosis was more severe in *Ws/Ws* rats than in the control littermates, suggesting that mast cells do not contribute to the development of interstitial fibrosis in this model. Rather, they may actually play a beneficial role in the process of fibrosis in the kidney.

METHODS

Animal model

Puromycin aminonucleoside (PAN) nephrosis model was induced in male mast cell–deficient *Ws/Ws* and their normal +/+ littermates (Japan SLC; Hamamatsu, Japan, $N = 12$ each), weighing 140 to 160 g, by the method of Jones et al [26], with slight modifications. In brief, left unilateral nephrectomy through a flank incision was performed on each rat under sodium pentobarbital (45 mg/kg body weight) anesthesia. Five days after the nephrectomy, the rats received an intraperitoneal (i.p.) injection of PAN (Sigma Chemical Co., St. Louis, MO, USA) dissolved in 0.9% saline (15 mg/mL) and given at a dose of 15-mg/100 g body weight. Second, third, and fourth doses of PAN (4.3 mg/100 g body weight, i.p.) were administered at 3, 4, and 5 weeks, respectively, after the initial dose. Control animals did not receive any surgical procedures or injections ($N = 10$ each). All animals were maintained on a standard rat diet and had free access to water throughout the course of the experiment. The animals were housed individually in metabolic cages to obtain 24-hour urine once every week. They were sacrificed sequentially at 2 ($N = 5$ each) and 6 weeks ($N = 5$ each except for $N = 4$ for PAN-injected *Ws/Ws* rats; see below) after the initial dose of PAN, namely, 1 week after the first and the last injections, respectively. Three of the PAN-injected *Ws/Ws* rats and 2 of the PAN-injected +/+ rats died of chronic renal failure by 6 weeks. These rats were found dead in their cages in the morning, and thus their kidneys could not be used for histologic studies. These animals were excluded from the subsequent analysis. At sacrifice, blood samples were collected by heart puncture under anesthesia with diethylether. The kidneys were perfused via the abdominal aorta with ice-cold saline, and pieces of renal tissues were fixed in 10% buffered formalin or periodate-lysine-paraformaldehyde (PLP) solution. Pieces of renal cortex were also used for RNA preparation and hydroxyproline analysis (see below). Urinary protein was quantified by the biuret method. Levels of blood urea nitrogen (BUN) were measured with a kit designed for clinical use (Wako Pure Chemical Industries, Osaka, Japan).

Kidney tissue preparation

The kidney tissues fixed in 10% buffered formalin were embedded in paraffin, sectioned, and stained with hematoxylin and eosin, periodic acid-Schiff (PAS), or Masson trichrome. The degree of interstitial fibrosis was semiquantitatively analyzed by inspection of Masson trichrome–stained sections and graded on a scale of 0 to 3 as follows: (*0*), no apparent damage; (*1*) mild damage, with lesions involving less than 5% of the cortex; (*2*) moderate damage, involving 5% to 20% of the cortex; and (*3*) severe damage, involving more than 20% of the cortex. Pieces for cryostat sectioning were fixed in PLP solution for 4 hours, washed several times in phosphate-buffered saline (PBS) containing 7% sucrose, embedded in Tissue-Tek OCT compound (Sakura Finetek, Torrance, CA, USA), and snap-frozen.

Immunohistochemical study

To block endogenous peroxidase activity, we treated sections of frozen or paraffin-embedded kidney tissues with methanol containing 0.6% hydrogen peroxide for 15 minutes and then washed them with PBS. They were stained by the standard avidin-biotin peroxidase technique with sheep antirat mast cell protease (RMCP) I (mast cell–specific antibody; Moredun, Scotland, UK), mouse monoclonal antibody ED-1 (specific for rat monocytes/macrophages), W3/25 ($CD4^+$ cells), or OX8 ($CD8^+$ cells) at 4°C overnight. The sections were incubated with the corresponding second antibodies, biotinylated donkey antisheep IgG or horse antimouse IgG, and stained with the reagents of an ABC staining kit (Vector Laboratories, Inc., Burlingame, CA, USA). Sections were also stained with horseradish peroxidase–conjugated mouse antihuman α-smooth muscle actin (α–SMA, a marker for myofibroblasts) monoclonal antibody (Dako Corp., Carpinteria, CA, USA). All sections were then developed with 3, 3′-diaminobenzidine solution as chromogen and counterstained with methylgreen. With the aid of a 10 × 10 eyepiece grid, the numbers of monocytes/macrophages, $CD4^+$, and $CD8^+$ cells in the interstitium were counted manually in 6 random nonoverlapping cortical fields (×400) of sections made from each experimental animal. RMCP I–positive interstitial mast cells were also counted in 20 random cortical fields (×100). The results of cell counting were expressed as the number per square millimeter.

Cell cultures

A cell line of renal fibroblasts (NRK49F) derived from rat kidney was obtained from The European

Table 1. Nucleotide sequences of the polymerase chain reaction (PCR) primers, the expected sizes of the amplified products, annealing temperature, and cycle numbers of PCR reactions

Primers			Product	Annealing temperature	Cycles
RMCP II	5′ primer	5′-ACGAAAGTTACAACTCCGTTC-3′	475 bp	60°C	32
	3′ primer	5′-GTGTCTCAAGCAGGTCAGG-3′			
RMCP V	5′ primer	5′-GTCTATAACCGTCCTCCTAG-3′	381 bp	54°C	38
	3′ primer	5′-TTTTGCATCTTCTTGGGGTTG-3′			
RMCP VIII	5′ primer	5′-GGCCATCCTACCAGTCAACAC-3′	341 bp	60°C	30
	3′ primer	5′-CACCATTGAGTTGAGCTTTGCG-3′			
GAPDH	5′ primer	5′-GGGAGCCAAAAGGGTCATCATCTC-3′	516 bp	64°C	18
	3′ primer	5′-CCATGCCAGTGAGCTTCCCGTTC-3′			

All of the PCR reactions were performed as described in the Methods section.

Collection of Cell Cultures (Salisbury, UK) and maintained in Dulbecco's modified Eagle's medium (Invitrogen, Grand Island, NY, USA) supplemented with 10% fetal calf serum (FCS), glutamine, and nonessential amino acid equilibrated with 5% CO_2-95% air at 37°C. For experiments, cells grown to 80% confluence in 100-mm dishes were exposed to fresh medium with or without 100 μg/mL heparin (sodium salt; Sigma) for 6 hours and then used for RNA preparation.

Reverse transcription-polymerase chain reaction (RT-PCR)

Total RNA fractions were prepared from pieces of renal cortex or cultured cells by the guanidinium thiocyanate-phenol-chloroform method [27], and 5 μg of RNA was reverse-transcribed by use of oligo(dT) primers in 20 μL of buffer as previously described [28]. For the analysis of levels of mRNA for RMCPs II, V, and VIII, 1 μL of this reaction mixture containing the cDNA was amplified by PCR in 50 μL of 10 mmol/L Tris-HCl (pH 9.0) containing 50 mmol/L KCl, 1.5 mmol/L $MgCl_2$, 5′ and 3′ primers (Table 1), and Taq DNA polymerase (Promega, Madison, WI, USA). Aliquots were electrophoresed on a 2% agarose gel and visualized with ethidium bromide under ultraviolet illumination. For the quantitative measurement of cytokine mRNA levels, real-time PCR was performed by using an ABI PRISM 7700 Sequence Detector and TaqMan® Pre-Developed Assay Reagents for Gene Expression Quantification System (Applied Biosystems, Foster City, CA, USA). Using multiple reporter dyes, we assayed the mRNA levels of each cytokine and endogenous control (GAPDH) in the same tube and expressed cytokine mRNA levels as the ratio relative to the endogenous control.

Hydroxyproline analysis

The amount of hydroxyproline in the renal cortex was measured according to Kivirikko et al [29] as an index of collagen content. At sacrifice, pieces of renal cortex for the hydroxyproline assay were weighed, snap-frozen in liquid nitrogen, and stored at −80°C for subsequent use. The samples were hydrolyzed in 1 mL of 6N hydrochloric acid at 110°C for 18 hours in tightly capped tubes. After the hydrolysates had been neutralized with sodium hydroxide, their hydroxyproline content was assessed colorimetrically at 560 nm with *p*-dimethylaminobenzaldehyde. Results were expressed as ng per mg wet renal cortex.

Statistical analysis

All values were expressed as the mean ± SD. Data were analyzed by the Mann-Whitney *U* test, and a difference with a value of $P < 0.05$ was considered to be statistically significant.

RESULTS

PAN nephrosis in *Ws/Ws* and +/+ rats

In PAN nephrosis model induced by uninephrectomy and subsequent administration of PAN, increases in urinary protein excretion and BUN level were observed in both mast cell–deficient *Ws/Ws* and their control (+/+) littermates; there was no difference in either parameter between the two groups (Fig. 1). At 6 weeks, the level of urinary protein excretion markedly decreased because of the loss of functioning nephrons (end-stage renal failure).

Renal fibrosis induced in *Ws/Ws* and +/+ rats by PAN

Interstitial fibrosis occurred in both PAN-treated *Ws/Ws* and +/+ rats at 2 weeks at the border of the cortex-medulla. A significant expansion of the fibrotic area was observed at 6 weeks in both strains. Unexpectedly however, the fibrosis was more severe in the *Ws/Ws* rats than in their +/+ littermates (Fig. 2). No obvious fibrosis was observed in the control animals. The magnitude of fibrosis was semiquantitatively determined with light microscopy (Fig. 3). The degree of fibrosis was similar in both groups at 2 weeks, but was greater in *Ws/Ws* rats than in +/+ rats at 6 weeks.

To confirm these histologic results, we measured the hydroxyproline content in the renal cortex (Fig. 4). At 2 weeks, although the content of this collagen marker

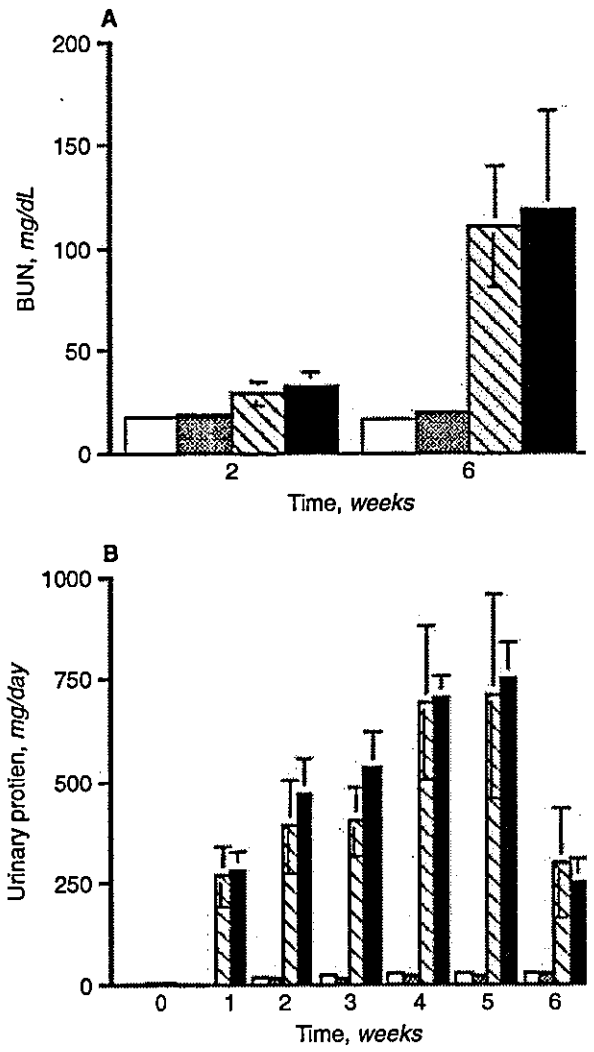

Fig. 1. Clinical course of puromycin aminonucleoside (PAN) nephrosis in *Ws/Ws* and +/+ rats. Blood urea nitrogen (*A*), urinary protein excretion (*B*). Control +/+ (□); Control *Ws/Ws* (■); PAN-treated +/+ (▨); PAN-treated *Ws/Ws* rats (■).

in PAN-treated animals was slightly higher than that in control animals, the difference was not statistically significant; and the level was similar in PAN-treated *Ws/Ws* and +/+ rats. At 6 weeks, the content was significantly greater in PAN-treated animals than in control animals. Moreover, the level in the PAN-treated *Ws/Ws* rats was significantly higher than that in the PAN-treated +/+ rats. Thus, the fibrotic changes in the interstitium assessed by both histologic and biochemical methods were greater in *Ws/Ws* rats than in their +/+ littermates.

Interstitial mast cells in PAN-induced nephrosis

Mast cells were immunohistochemically identified by their immunoreactivity, indicating the presence of RMCP I, a specific marker for mast cells [30, 31]. An almost complete absence of mast cells in the skin of *Ws/Ws* rats was confirmed by immunostaining for RMCP I (data not shown). Practically no mast cells were detectable in the kidney of control *Ws/Ws* and +/+ rats. However, in the kidney tissues of PAN-treated +/+ rats, mast cells were observed in the interstitium, where they showed a scattered distribution (Fig. 5A). Most were localized in the peritubular region (Fig. 5B).

To confirm the increase in the number of mast cells in the kidney, we also examined mRNA levels of other specific markers for mast cells (i.e., RMCPs II, V, and VIII). By RT-PCR analysis, mRNAs for all of these proteases were consistently found in disease-induced rats, but not in control rats, by the experimental procedures used (Fig. 6).

The time-kinetics of the number of interstitial mast cells determined by immunohistochemistry is illustrated in Figure 7. After administration of PAN, the number of mast cells increased significantly in both *Ws/Ws* and +/+ rats, but was lower in the former than in the latter. While the number of mast cells gradually increased in PAN-treated +/+ rats with the expansion of the interstitial fibrosis, the number in PAN-treated *Ws/Ws* rats decreased with the continued expansion. The number in PAN-treated *Ws/Ws* rats was one half at 2 weeks and one fifth at 6 weeks compared with that in the PAN-treated +/+ rats.

Other interstitial cells in PAN-induced nephrosis

Because thymocytes are *c-kit*–positive cells, the defect in *c-kit* carried by *Ws/Ws* rats could potentially affect T-cell development, although there have been no reports showing such T-cell deficits. It is also known that myofibroblasts express *c-kit* [32]. To clarify the influence of the *c-kit* deletion in these types of cell in the kidney of *Ws/Ws* rats, we examined the levels of monocytes/macrophages, CD4–, CD8–, and α–SMA–positive cells in the interstitium (Table 2). Low numbers of these types of cells were detected in the interstitium of the control animals. After the disease induction, their numbers increased in both *Ws/Ws* and +/+ rats, but there were no differences in them between the two strains. Most of the monocyte/macrophages and CD4– and CD8– positive cells were found in the interstitial lesion in clusters, especially in the area around glomeruli and disrupted tubuli, and the localization was different from that of the mast cells.

Cytokine mRNA levels in renal cortex

To investigate the possible mechanism for the increase in fibrosis in these *Ws/Ws* rats, we measured mRNA levels of cytokines that might affect the progression of fibrosis. As shown in Figure 8, the levels of mRNA for two potentially profibrotic cytokines, TGF-β and interleukin (IL)-4,

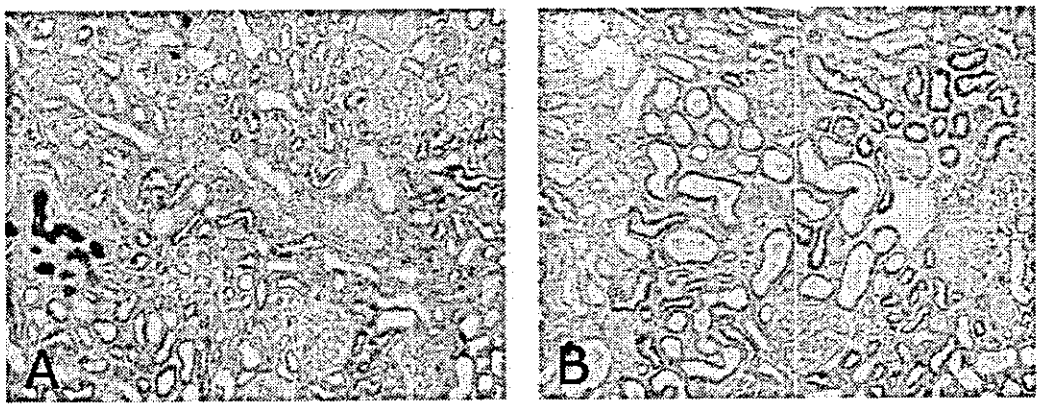

Fig. 2. Representative histologic changes in the kidney in puromycin aminonucleoside (PAN) nephrosis. Kidney tissues were obtained at 6 weeks from PAN-treated +/+ rats (*A*) and PAN-treated *Ws/Ws* rats (*B*). Masson-trichrome staining. Original magnification ×100.

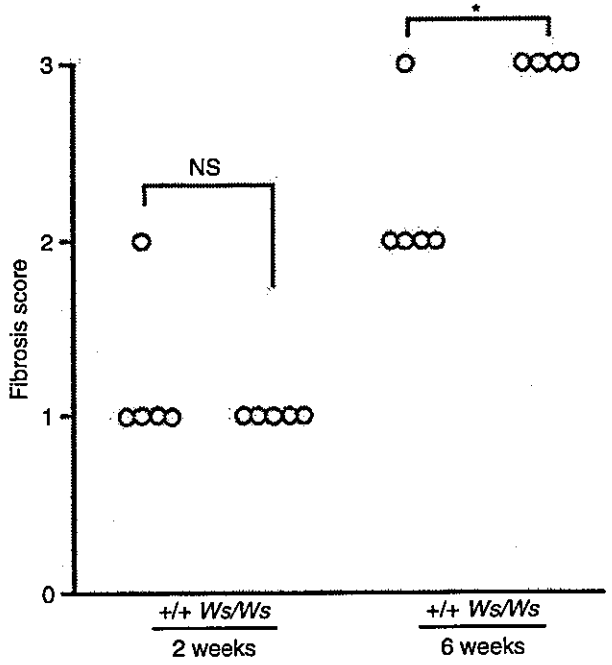

Fig. 3. Semiquantification of the fibrotic interstitium in puromycin aminonucleoside (PAN) nephrosis. Kidney tissues were obtained at 2 and 6 weeks from PAN-treated +/+ and *Ws/Ws* rats. $^*P < 0.05$.

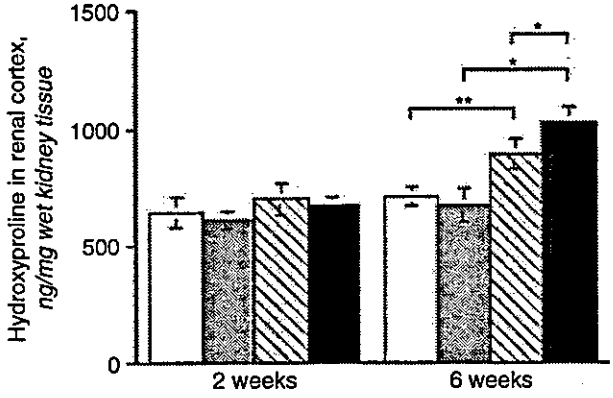

Fig. 4. Hydroxyproline content in renal cortex of rats with puromycin aminonucleoside (PAN) nephrosis. Control +/+ (□); control *Ws/Ws* (■); PAN-treated +/+ (▨); PAN-treated *Ws/Ws* rats (■). $^*P < 0.05$; $^{**}P < 0.01$.

were higher in the *Ws/Ws* rats than in the +/+ ones. The differences between the two groups in the level of TGF-β mRNA at 2 weeks, and in that of IL-4 mRNA at 6 weeks, were statistically significant. There were no differences in mRNA levels of IL-2, IL-10, and interferon (IFN)-γ in the renal cortex between the two strains. These results suggest that the enhanced production of TGF-β and/or IL-4 in *Ws/Ws* rats may have caused the enhanced fibrosis in the kidney.

Effect of heparin on the expression of TGF-β1 mRNA in renal fibroblast in culture

Although mast cells have been shown to produce TGF-β and IL-4 in culture [9], they also produce other cytokines and factors that may modulate the production of these cytokines by other types of cells. Heparin is a major component stored in secretory granules of mast cells and is known to influence cytokine production in culture [33]. Therefore, using a cell line of interstitial fibroblasts derived from normal rat kidney, we investigated if heparin could influence the production of TGF-β in culture. As shown in Figure 9, the expression of TGF-β mRNA in renal fibroblast was inhibited by heparin.

DISCUSSION

In progressive human glomerular diseases, regardless of their type, the number of interstitial mast cells

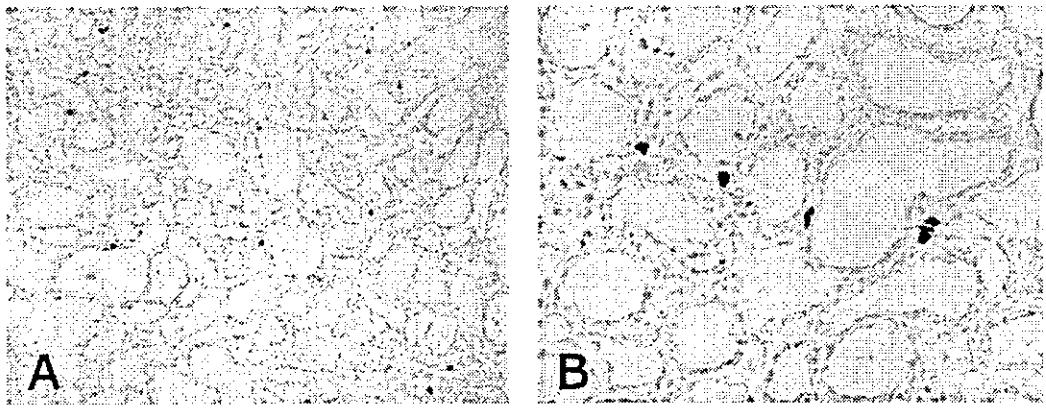

Fig. 5. Immunostaining for rat mast cell protease (RMCP) I, a specific marker for mast cell, in puromycin aminonucleoside (PAN) nephrosis. Representative kidney sections obtained at 6 weeks from PAN-treated +/+ rats are shown. RMCP I-positive cells with a scattered distribution are seen in the interstitium (*A*). These cells are mostly located in the peritubular region (*B*). Original magnification, ×100 (A) and ×200 (B).

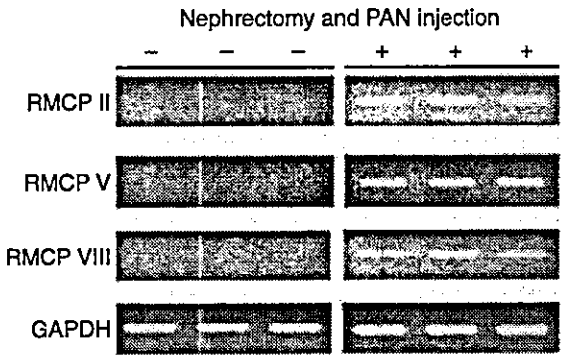

Fig. 6. Expression of mRNA for rat mast cell proteases (RMCPs) II, V, and VIII. RNA extracted from 3 animals of each group [2-week puromycin aminonucleoside (PAN)-treated +/+ rats and control +/+ rats] was used for reverse transcription-polymerase chain reaction (RT-PCR) analysis. Each lane represents the mRNA expression of each animal. The GAPDH band is shown as the internal control.

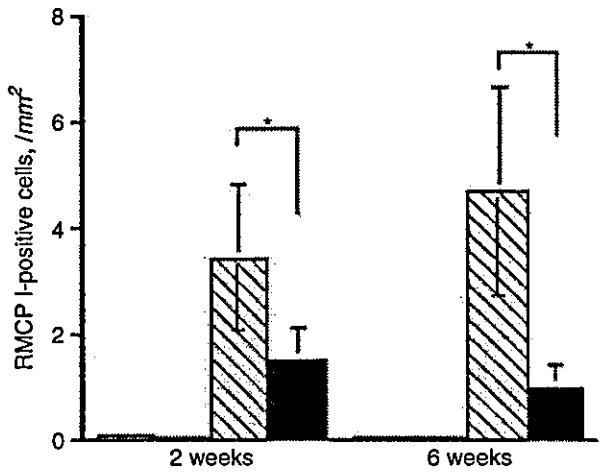

Fig. 7. Numbers of interstitial rat mast cell protease (RMCP) I-positive cells in puromycin aminonucleoside (PAN) nephrosis. Control +/+ (□); control *Ws/Ws* (■); PAN-treated +/+ (▨); PAN-treated *Ws/Ws* rats (■). $^*P < 0.05$.

increases as interstitial fibrosis expands [14, 15, 17]. The present study has demonstrated that in PAN nephrosis, a rat model of progressive glomerular disease, the number of interstitial mast cells also increased concomitant with the expansion of interstitial fibrosis. We also found that the number of interstitial mast cells increased in the crescentic glomerulonephritis model in Wistar Kyoto rats (our unpublished observations). These results indicate that, like in humans, mast cells accumulate in the interstitial area in progressive renal diseases in rats when interstitial fibrosis develops.

Because PAN nephrosis can be induced in any strain of rat, using mast cell–deficient *Ws/Ws* rats, we then investigated the suggested causal link between mast cell accumulation and interstitial fibrosis. Unexpectedly, interstitial fibrosis was markedly worse in these rats. Although mast cells were not completely absent in the diseased kidney of *Ws/Ws* rats, their number at 6 weeks in PAN-treated *Ws/Ws* rats was approximately one fifth of that in the PAN-treated control littermates. Because it was shown that the number of mast cells in the whole body of *Ws/Ws* rats is decreased by aging [23], we considered that the decrease in the number of interstitial mast cells from 2 to 6 weeks in the rats resulted from aging and is irrelevant to the development of interstitial fibrosis. The observed interstitial mast cells in the *Ws/Ws* rats may have resulted from the accumulation of the remaining small number of mast cells from other parts of the body [34]. In contrast, there were no differences between the two strains in the levels of interstitial T lymphocytes and myofibroblasts, two types of cell that could be affected by the *c-kit* gene mutation in *Ws/Ws* rats. Taken together, these results suggest that the reduction in the number of interstitial mast cells in *Ws/Ws* rats resulted in the exacerbation of interstitial fibrosis in this model.

Table 2. Interstitial cells in +/+ and *Ws/Ws* rats at 6 weeks

	Control		PAN nephrosis	
	+/+	*Ws/Ws*	+/+	*Ws/Ws*
ED-1 (monocytes/macrophages)[a]	83.8 ± 13.3	80.0 ± 10.6	570.0 ± 40.1	592.0 ± 46.3
W3/25 ($CD4^+$ cells)[a]	157.4 ± 14.4	165.8 ± 11.8	593.9 ± 42.4	580.0 ± 36.0
OX8 ($CD8^+$ cells)[a]	21.1 ± 10.3	16.6 ± 4.8	116.5 ± 12.7	112.8 ± 12.6
α-SMA (myofibroblast)[b]	1.2 ± 0.3	1.3 ± 0.3	11.6 ± 1.1	10.5 ± 3.3

α-SMA, alpha-smooth muscle actin.
[a]Data are the numbers of interstitial cells per mm^2 expressed as mean ± SD ($N = 5$).
[b]Data are % interstitial positive area expressed as mean ± SD ($N = 5$).

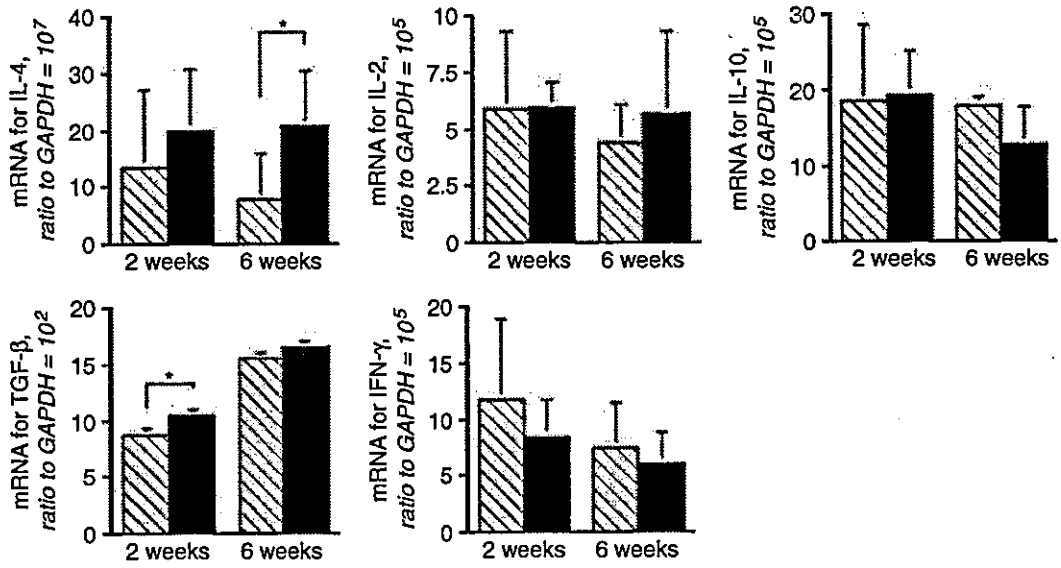

Fig. 8. Expression of cytokine mRNA levels in renal cortex of rats with puromycin aminonucleoside (PAN) nephrosis. Data are expressed as the ratio to the internal control. PAN-treated +/+ (▨); PAN-treated *Ws/Ws* rats (■). $^*P < 0.05$.

It was demonstrated earlier that myofibroblast proliferation is paralleled by or precedes the development of interstitial fibrosis in human and animal models [35], but the result of the present study is not consistent with those previous studies. It could be possible that there is some unknown effect that originated from the mutated *c-kit* gene that changed the functions of myofibroblasts in *Ws/Ws* rats. In addition, we cannot exclude the possibility that the mutated *c-kit* gene causes other abnormalities than mast cell deficiency, although there have been no reports so far that show such defects in *Ws/Ws* rats except for anemia in their early life [23].

Our present study using mast cell–deficient *Ws/Ws* is the first one to our knowledge to reveal the role of mast cells in renal fibrosis. There have been some earlier studies in which the involvement of mast cells in fibrosis of lung [36, 37], liver [36, 38], and skin [39, 40] was examined by using mast cell–deficient W/W^v mice and/or *Ws/Ws* rats. Some of these studies showed no difference in the magnitude of fibrosis between the mast cell–deficient animals and their control +/+ littermates, which suggested that mast cells do not appear to be necessary for the induction of fibrosis. In the present study, our histologic and biochemical analysis revealed that the fibrosis was more severe in *Ws/Ws* rats than in +/+ littermates at 6 weeks after the induction of PAN nephrosis. These data are consistent with other studies on lung [36, 37] and liver [36] fibrosis, which showed that the increase in the hydroxyproline content of the tissues of deficient animals was greater than that in control +/+ littermates.

The mechanism by which greater renal interstitial fibrosis occurred in *Ws/Ws* rats with PAN nephrosis is unclear. We investigated the possibility that levels of cytokines that potentially enhance directly or indirectly the progression of fibrosis are changed in *Ws/Ws* rats with PAN nephrosis. The cytokines tested in this study included Th1 and Th2 cytokines, the balance of which is suggested to affect fibrotic changes [41]. Our results showed that mRNA levels of TGF-β and IL-4 were higher in *Ws/Ws* rats than in controls in the PAN nephrosis model,

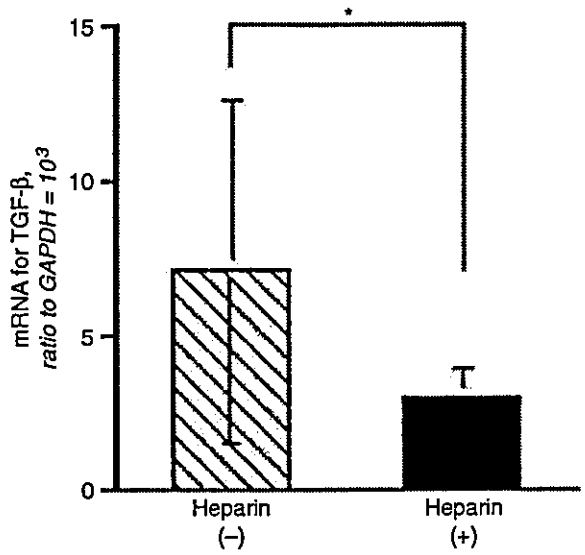

Fig. 9. Inhibition of expression of transforming growth factor (TGF)-β1 mRNA by heparin. Rat renal fibroblasts were cultured in the absence (▨) or presence (■) of heparin for 6 hours. Data are expressed as mean ± SD of 5 samples.

suggesting that the deficiency of mast cells (i.e., in *Ws/Ws* rats) may have caused an increase in their expression, resulting in more fibrosis in the *Ws/Ws* rats.

Mast cells contain a variety of mediators that have been shown to directly or indirectly affect the progression of fibrosis in tissues [42]. Although mast cells have been shown to produce TGF-β and IL-4 in culture [9], they also produce other cytokines and factors that may modulate cytokine production by other types of cells. Heparin, a major component stored in secretory granules of mast cells, was shown to have effects on cell proliferation [43] and cytokine production [33], both of which are involved in the pathogenesis of fibrosis. Heparin was also shown to inhibit DNA synthesis by human renal fibroblasts when added alone, although it enhanced DNA synthesis when added with tryptase, a proteolytic enzyme secreted by mast cells [44]. The present study demonstrated that heparin inhibited the gene expression of TGF-β, the most potent fibrogenic cytokine, in renal fibroblasts in culture. A recent study also demonstrated that heparin inhibited the production of TGF-β by cultured human proximal tubular epithelial cells, another source of the cytokine in diseased kidney [45]. Therefore, it is conceivable that heparin secreted from mast cells may inhibit TGF-β production by these cells in the diseased kidney and that this action may have contributed to the less fibrosis in the control +/+ littermates in the PAN nephrosis model. We also tested the effect of heparin on IL-4 production by these cells, but the production level was very low, and thus the effect of heparin could not be detected (our unpublished observation).

The results of the present study using mast cell–deficient animals seem to be in conflict with a suggested role of mast cells in renal diseases. The profibrogenic role of mast cells has been proposed mostly based on histologic observations of clinical samples and results of in vitro studies using cultured cells [14–20, 44]. However, the histologic studies only showed a correlation between the two phenomena, mast cell accumulation and fibrosis, and do not provide evidence of a causal link between them. In vitro studies, on the other hand, give data on the potential effects of mast cells or their secretory components on fibrosis, but do not provide information about the overall effect of mast cells. Even if whole components stored in mast cells or mast cells themselves are used in a culture system, one cannot provide all cells and extracellular circumstances of the kidney in the in vitro system. Further studies are needed to elucidate the role of mast cells in the mechanism of fibrosis, but we consider that experiments using animal models as well as intervention studies in humans will be necessary to assess the effect of mast cells as a whole on fibrosis.

In the kidney of the animal models of glomerular diseases we tested, mast cells were localized in a scattered distribution in the interstitium, whereas interstitial mononuclear cells (MNC), mostly consisting of monocytes/macrophages and T lymphocytes, were present in clusters. In human glomerular diseases on the other hand, mast cells were restricted to the area of interstitial fibrosis where only a few T lymphocytes and macrophages were concomitantly present, but were rarely found in the interstitial lesion where the influx of MNC was pronounced (our unpublished observations). This interstitial influx of MNC presumably precedes the interstitial fibrosis and is suggested to be involved in the mechanism of fibrotic changes [46]. Therefore, in consideration of these findings, together with the results of the present study, it is conceivable that mast cells are not involved in the development of fibrosis because of their absence in prefibrotic lesions in contrast to T lymphocytes or macrophages, but are attracted in fibrotic lesion and possibly participate in the attenuation or resolution of the fibrotic lesions. Unfortunately, in the rodent models it was rather difficult to discriminate prefibrotic lesions from established areas of fibrosis, probably because of the short duration and/or acute inflammation after the disease onset.

CONCLUSION

In the present study, we investigated the role of mast cells in the development of renal fibrosis by using mast cell–deficient rats. In human studies, mast cells are thought to be one of the cell types contributing to the interstitial fibrosis. However, it could be mentioned from our data that mast cells are not simply fibrogenic. Rather, they might have a potential to be protective or

ameliorative in this model and possibly in other models and also in humans.

ACKNOWLEDGMENTS

We are grateful to Dr. Takashi Oda, National Defense Medical College, for his advice concerning the hydroxyproline analysis. This work was supported in part by a Health Science Research Grant (Research on Specific Diseases) from the Ministry of Health and Welfare. Portions of this work were presented at the 2001 Annual Meeting of the American Society of Nephrology and reported in abstract form (*J Am Soc Nephrol* 12:711A, 2001).

Reprint requests to Dr. Yasuhiro Natori, Department of Clinical Pharmacology, Research Institute, International Medical Center of Japan, Toyama 1–21-1, Shinjuku-ku, Tokyo 162–8655, Japan.
E-mail: natoriya@ri.imcj.go.jp

REFERENCES

1. Pesci A, Bertorelli G, Gabrielli M: Mast cells in fibrotic lung disorders. *Chest* 103:989–996, 1993
2. Pesci A, Majori M, Piccili ML, *et al*: Mast cells in bronchiolitis obliterans organizing pneumonia: Mast cell hyperplasia and evidence for extracellular release of tryptase. *Chest* 110:383–391, 1996
3. Murata K, Okudaira M, Akashio K: Mast cells in human liver tissue. Increased mast cell number in relation to the components of connective tissue in the cirrhotic process. *Acta Derm Venereol* 73:157–165, 1973
4. Armbrust T, Batusic D, Ringe B, *et al*: Mast cell distribution in human liver disease and experimental rat liver fibrosis: Indications for mast cell participation in development of liver fibrosis. *J Hepatol* 26:1042–1054, 1997
5. Hawkins RA, Claman HN, Clark RAF, *et al*: Increased dermal mast cell populations in progressive systemic sclerosis: A link in chronic fibrosis? *Ann Intern Med* 102:182–186, 1985
6. Rothe MJ, Nowak M, Kerdel FA: The mast cell in health and disease. *J Am Acad Dermatol* 23:615–624, 1990
7. Craig SS, DeBlois G, Schwartz LB: Mast cells in human keloid, small intestine, and lung by an immunoperoxidase technique using a murine monoclonal antibody against tryptase. *Am J Pathol* 124:427–435, 1986
8. Schwartz LB: Mast cells: Function and contents. *Curr Opin Immunol* 6:91–97, 1994
9. Gordon JR, Burd PR, Galli SJ: Mast cells as a source of multifunctional cytokines. *Immunol Today* 11:458–464, 1990
10. Ruoss SJ, Hartmann T, Caughey GH: Mast cell tryptase is a mitogen for cultured fibroblasts. *J Clin Invest* 88:493–499, 1991
11. Gruber BL, Kew RR, Jelaska A, *et al*: Human mast cells activate fibroblasts: Tryptase is a fibrogenic factor stimulating collagen messenger ribonucleic acid synthesis and fibroblast chemotaxis. *J Immunol* 158:2310–2317, 1997
12. Gordon JR, Galli SJ: Promotion of mouse fibroblast collagen gene expression by mast cells stimulated via the Fc epsilon RI. Role for mast cell-derived transforming growth factor beta and tumor necrosis factor alpha. *J Exp Med* 180:2027–2037, 1994
13. Thompson HL, Burbelo PD, Gabriel G, *et al*: Murine mast cells synthesize basement membrane components. A potential role in early fibrosis. *J Clin Invest* 87:619–623, 1991
14. Ehara T, Shigematsu H: Contribution of mast cells to the tubulointerstitial lesions in IgA nephritis. *Kidney Int* 54:1675–1683, 1998
15. Hiromura K, Kurosawa M, Yano S, *et al*: Tubulointerstitial mast cell infiltration in glomerulonephritis. *Am J Kidney Dis* 32:593–599, 1998
16. Roberts IS, Brenchley PE: Mast cells: The forgotten cells of renal fibrosis. *J Clin Pathol* 53:858–862, 2000
17. Toth T, Toth-Jakatics R, Jimi S, *et al*: Mast cells in rapidly progressive glomerulonephritis. *J Am Soc Nephrol* 10:1498–1505, 1999
18. Ruger BM, Hasan Q, Greenhill NS, *et al*: Mast cells and type VIII collagen in human diabetic nephropathy. *Diabetologia* 39:1215–1222, 1996
19. Lajoie G, Nadasdy T, Laszik Z, *et al*: Mast cells in acute cellular rejection of human renal allografts. *Mod Pathol* 9:1118–1125, 1996
20. Yamada M, Ueda M, Naruko T, *et al*: Mast cell chymase expression and mast cell phenotypes in human rejected kidneys. *Kidney Int* 59:1374–1381, 2001
21. Risdon RA, Sloper JC, de Wardener HE: Relationship between renal function and histological changes found in renal-biopsy specimens from patients with persistent glomerular nephritis. *Lancet* 2:363–366, 1968
22. Cameron JS: Tubular and interstitial factors in the progression of glomerulonephritis. *Pediatr Nephrol* 6:292–303, 1992
23. Niwa Y, Kasugai T, Ohno K, *et al*: Anemia and mast cell depletion in mutant rats that are homozygous at "white spotting (Ws)" locus. *Blood* 78:1936–1941, 1991
24. Tsujimura T, Hirota S, Nomura S, *et al*: Characterization of *Ws* mutant allele of rats: A 12-base deletion in tyrosine kinase domain of *c-kit* gene. *Blood* 78:1942–1946, 1991
25. Onoue H, Maeyama K, Nomura S, *et al*: Absence of immature mast cells in the skin of Ws/Ws rats with a small deletion at tyrosine kinase domain of the c-kit gene. *Am J Pathol* 142:1001–1007, 1993
26. Jones CL, Buch S, Post M, *et al*: Pathogenesis of interstitial fibrosis in chronic purine aminonucleoside nephrosis. *Kidney Int* 40:1020–1031, 1991
27. Chomczynski P, Sacchi N: Single-step method of RNA isolation by acid guanidinium thiocyanate-phenol-chloroform extraction. *Anal Biochem* 162:156–159, 1987
28. Ou ZL, Natori Y, Doi N, *et al*: Competitive reverse transcription-polymerase chain reaction for determination of rat CC and C chemokine mRNAs. *Anal Biochem* 261:227–229, 1998
29. Kivirikko KI, Laitinen O, Prockop DJ: Modifications of a specific assay for hydroxyproline in urine. *Anal Biochem* 19:249–255, 1967
30. Gibson S, Miller HR: Mast cell subsets in the rat distinguished immunohistochemically by their content of serine proteinases. *Immunology* 58:101–104, 1986
31. Gibson S, Mackeller A, Newlands GF, *et al*: Phenotypic expression of mast cell granule proteinases. Distribution of mast cell proteinases I and II in the rat digestive system. *Immunology* 62:621–627, 1987
32. Powell DW, Mifflin RC, Valentich JD, *et al*: Myofibroblasts. I. Paracrine cells important in health and disease. *Am J Physiol* 277:C1–9, 1999
33. Weigert C, Brodbeck K, Haring HU, *et al*: Low-molecular-weight heparin prevents high glucose- and phorbol ester-induced TGF-beta 1 gene activation. *Kidney Int* 60:935–943, 2001
34. Tei H, Kasugai T, Tsujimura T, *et al*: Characterization of cultured mast cells derived from *Ws/Ws* mast cell-deficient rats with a small deletion at tyrosine kinase domain of *c-kit*. *Blood* 83:916–925, 1994
35. Remuzzi G, Bertani T: Pathophysiology of progressive nephropathies. *N Engl J Med* 339:1448–1456, 1998
36. Okazaki T, Hirota S, Xu ZD, *et al*: Increase of mast cells in the liver and lung may be associated with but not a cause of fibrosis: Demonstration using mast cell-deficient Ws/Ws rats. *Lab Invest* 78:1431–1438, 1998
37. Mori H, Kawad K, Zhang P, *et al*: Bleomycin-induced pulmonary fibrosis in genetically mast cell-deficient WBB6F1-W/Wv mice and mechanism of the suppressive effect of tranilast, an antiallergic drug inhibiting mediator release from mast cells, on fibrosis. *Int Arch Allergy Appl Immunol* 95:195–201, 1991
38. Sugihara A, Tsujimura T, Fujita Y, *et al*: Evaluation of role of mast cells in the development of liver fibrosis using mast cell-deficient rats and mice. *J Hepatol* 30:859–867, 1999
39. Everett ET, Pablos JL, Harley RA, *et al*: The role of mast cells in the development of skin fibrosis in tight-skin mutant mice. *Comp Biochem Physiol A Physiol* 110:159–165, 1995
40. Yamamoto T, Takahashi Y, Takagawa S, *et al*: Animal model of sclerotic skin. II. Bleomycin induced scleroderma in genetically mast cell deficient WBB6F1-W/Wv mice. *J Rheumatol* 26:2628–2634, 1999
41. Lukacs NW, Hogaboam C, Chensue SW, *et al*: Type 1/type 2 cytokine paradigm and the progression of pulmonary fibrosis. *Chest* 120:5S–8S, 2001
42. Metcalfe DD, Baram D, Mekori YA: Mast cells. *Physiol Rev* 77:1033–1079, 1997

43. Del Vecchio PJ, Bizios R, Holleran LA, *et al*: Inhibition of human scleral fibroblast proliferation with heparin. *Invest Ophthalmol Vis Sci* 29:1272–1276, 1988
44. Kondo S, Kagami S, Kido H, *et al*: Role of mast cell tryptase in renal interstitial fibrosis. *J Am Soc Nephrol* 12:1668–1676, 2001
45. Yard BA, Chorianopoulos E, Herr D, *et al*: Regulation of endothelin-1 and transforming growth factor-beta1 production in cultured proximal tubular cells by albumin and heparan sulphate glycosaminoglycans. *Nephrol Dial Transplant* 16:1769–1775, 2001
46. Muller GA, Markovic-Lipkovski J, Frank J, *et al*: The role of interstitial cells in the progression of renal diseases. *J Am Soc Nephrol* 2:S198–S205, 1992